

Negative Normal Stress Elasticity of Emulsions of Viscous Drops at Finite Inertia

Xiaoyi Li and Kausik Sarkar

Department of Mechanical Engineering, University of Delaware, Newark, Delaware 19716, USA

(Received 13 June 2005; published 15 December 2005)

The relation between the normal stress and the imposed strain for a Newtonian emulsion in an oscillating extensional flow is computed at finite Reynolds numbers using numerically simulated drop geometry. The interfacial stress was determined using Batchelor's formalism. In the presence of inertia, the phase between the stress and the strain deviates from Stokes's flow, and leads to a negative elastic modulus at small frequencies. The results are explained by a mass-spring-dashpot model.

DOI: [10.1103/PhysRevLett.95.256001](https://doi.org/10.1103/PhysRevLett.95.256001)

PACS numbers: 83.50.-v, 47.10.+g, 47.11.-tj, 82.70.Kj

An emulsion containing small droplets of one liquid suspended in another, even if both are viscous, displays an effective macroscale viscoelastic response. The elasticity emanates from the interfacial tension acting at the boundary between the deforming drops and the continuous phase [1]. For a spherical drop the interfacial tension contributes to zero net stress. But a drop deformed in an imposed flow gives rise to excess stress. The phase lag between the imposed flow and the drop response determines the division of this excess stress into viscous and elastic components. Starting with Taylor [2], many analytical models have been developed to describe the drop deformation in simple shear or extension [3]. Batchelor [4] developed a theory for the stress system of suspensions or emulsions providing an expression for the effective stress as a function of positions and shapes of the drops.

Because of the small size R of the suspended drops, and the slow velocity U encountered in emulsion flows, the Reynolds number $\rho UR/\mu$ (μ is the viscosity, ρ density) is often small. Consequently, experimental investigations of drop deformation and emulsion rheology have been restricted to creeping flows; the inertialess Stokes limit is invoked in the analysis. However, there are numerous high speed industrial flows, where the drop Reynolds number can be $O(1)$ or higher or unsteady effects become prominent. The presence of inertia alters the phase lag between the imposed flow and the drop response [5], leading, as we will see, to negative values for normal stress storage modulus for a range of frequency.

Negative modulus does not violate any physical law. Recently, "metamaterials" with negative refraction for electromagnetic wave propagation have attracted a lot of attention [6]. These materials are manufactured by machining designed microstructures such as an array of wire elements into a substrate material. The dimensions of the embedded elements are much smaller than the wavelength and play an identical role to that of droplets in an emulsion, both leading to negative effective properties. The mechanism behind the negative refraction emerges from the frequency response of individual wire elements, just as the anomalous elasticity for emulsion does from the frequency response of droplets. The analogy is further de-

lined by the model for the drop contribution to the stress below. It should be mentioned that, in steady shear, negative first normal stress has been predicted for liquid crystalline polymers due to director tumbling motion [7] and also was recently measured in attractive emulsion [8] and nanotube suspension [9]. Inertia has recently been demonstrated to result in the same effect for viscous emulsion [10].

We numerically investigated the rheology of a dilute emulsion of viscous drops in an oscillating extensional flow of a four-roll mill [2,11]:

$$\begin{pmatrix} u \\ v \\ w \end{pmatrix} = \dot{\epsilon}_0 \cos(\omega t) \begin{pmatrix} 1 & 0 & 0 \\ 0 & -1 & 0 \\ 0 & 0 & 0 \end{pmatrix} \begin{pmatrix} x \\ y \\ z \end{pmatrix},$$

where $\dot{\epsilon}_0$ is the amplitude of the strain rate, and ω the frequency of oscillation (Fig. 1). Such flows are important in processing and mixing of polymer blends and because of absence of rotation in the velocity gradient, they provide a direct means of assessing the effects of stretching on the emulsion. The flow is governed by the Navier-Stokes

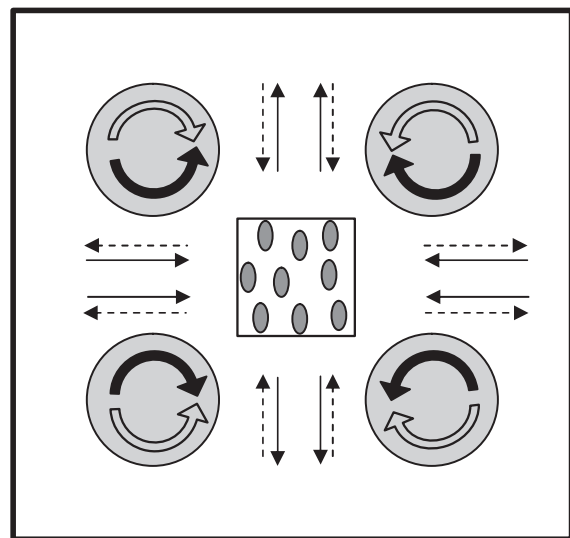


FIG. 1. Emulsion of drops in an oscillating extensional flow generated by a four-roll mill.

equation in both the drop and the continuous phase; the velocity and the tangential stresses are continuous at the interface and the normal stress experiences a jump due to the interfacial tension [12]. For a dilute emulsion the drops are too far apart to interact with each other, and each is subjected to the imposed oscillating extensional flow. We simulate a single drop in such a flow using a front tracing finite difference technique. The governing nondimensional parameters, Reynolds number $Re = \rho \dot{\epsilon}_0 R^2 / \mu$, inverse capillary number $k = Ca^{-1} = \Gamma / (\mu \dot{\epsilon}_0 R)$ (Γ is the interfacial tension), and Strouhal number (nondimensional frequency) $St = \omega / \dot{\epsilon}_0$ are varied fixing the density and the viscosity ratios to unity.

The simulation results on the drop dynamics have been reported before [5]. As shown there, the drop undergoes squeezing and stretching in orthogonal directions with the imposed flow, maintains an approximately ellipsoidal shape and reaches a steady-oscillating state with the same frequency as the imposed flow following a short transient. In Fig. 2, the top view (z direction) of the drop shape in the steady-oscillating state is shown together with the flow field in a plane through the center of the drop. The second and the fourth frames show significant drop deformation even though they correspond to zero strain rate, indicating that the drop responds to the flow with a phase difference. At finite inertia, the phase difference becomes anomalous in that the drop leads the flow field giving rise to a negative phase lag compared to the flow strain rate. Indeed, in Fig. 2 (case of $Re = 1.0$, $k = 200$, $St = 5\pi$) the drop deformation in the second frame is leading the flow stretching in the third frame. Such a phenomenon indicates that the drop-induced excess interfacial stress would also show an anomalous behavior, which is elucidated in this Letter.

The volume-averaged stress for a dilute emulsion of identical drops is given by Batchelor as [4,13]

$$\begin{aligned} \boldsymbol{\sigma}_{\text{ave}} &= \frac{1}{V} \int_V \boldsymbol{\sigma} dV = -P_{\text{ave}} \mathbf{I} + \boldsymbol{\tau}_{\text{ave}} + \boldsymbol{\sigma}_{\text{excess}}, \\ \boldsymbol{\sigma}_{\text{excess}} &= \Phi \boldsymbol{\sigma}_{\text{excess}}^d = -\Gamma \Phi \mathbf{q}^d, \\ \mathbf{q}^d &= \frac{1}{V_d} \int_{A_d} \left(\mathbf{nn} - \frac{\mathbf{I}}{3} \right) dA, \end{aligned} \quad (1)$$

where V is the averaging volume with m droplets within, A_d and V_d are the area and the volume of a single drop, and $\Phi = mV_d/V$ is the droplet volume fraction. P_{ave} is the isotropic part of the average stress, \mathbf{I} is the identity tensor, and $\boldsymbol{\tau}_{\text{ave}}$ is the deviatoric part excluding the contribution from the drop interface. $\boldsymbol{\sigma}_{\text{excess}}$ is the interfacial contribu-

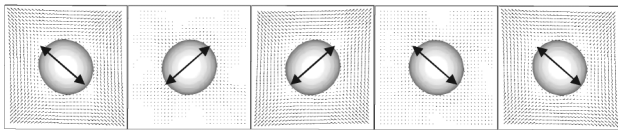


FIG. 2. Drop shape in one period in steady state; $k = 200$, $St = 5\pi$, $Re = 1.0$.

tion; \mathbf{q}^d , the interface tensor, is determined by the drop shape, \mathbf{n} the outward unit normal vector at the drop interface. In a dilute emulsion the contributions of each drop to the bulk stress are independent, giving a linear variation with Φ . The single drop excess stress $\boldsymbol{\sigma}_{\text{excess}}^d$ nondimensionalized by $\mu \dot{\epsilon}_0$ is expressed as $\boldsymbol{\Sigma}_{\text{excess}}^d = -\Gamma \mathbf{q}^d / (\mu \dot{\epsilon}_0) = -kR \mathbf{q}^d$. The interface tensor is computed integrating over the simulated drop surface. The oscillating extensional flow gives rise to equal positive and negative flow strains along the extensional axes: $\epsilon = \int \dot{\epsilon} dt = \dot{\epsilon}_0 / \omega \sin \omega t = (1/St) \sin(t' St)$, where $t' = t \dot{\epsilon}_0$ is the nondimensional time, and $\epsilon_0 = \dot{\epsilon}_0 / \omega = 1/St$ is the strain amplitude. Note that the strain by definition lags the strain rate by $\pi/2$.

The normal stress difference $\Sigma_{22}^d - \Sigma_{11}^d$ is plotted in Fig. 3 for different nondimensional frequencies (Strouhal numbers) at Reynolds number 0.1 and 1.0. For the lower Reynolds number case, the stress is viscous, i.e., in phase with the strain rate, and leads the imposed strain, by $\pi/2$ at low frequency ($St = \pi$). With increasing frequency, the stress becomes progressively elastic. It becomes in phase

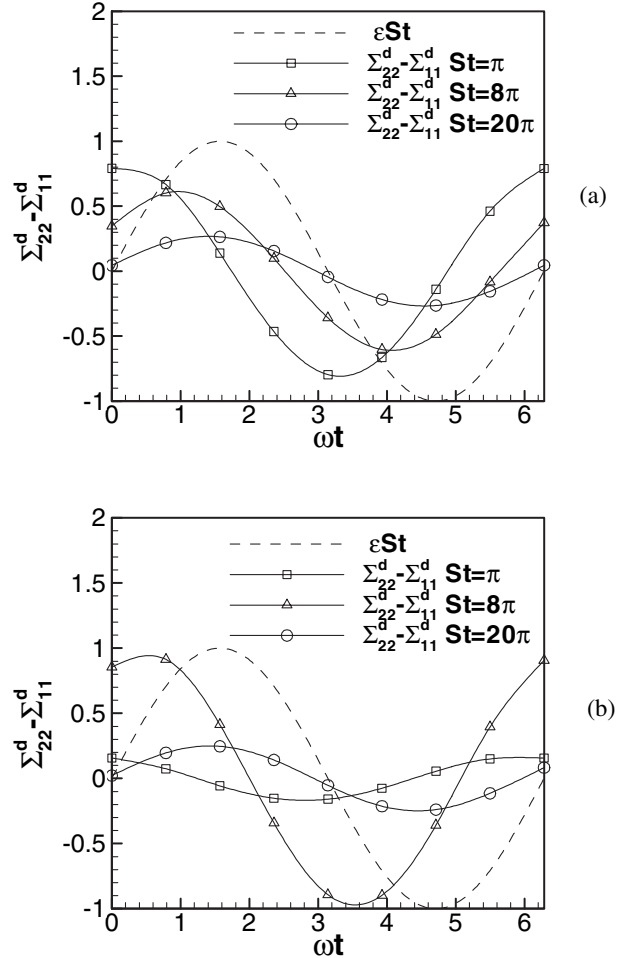


FIG. 3. Flow strain ϵSt and interfacial stress difference $\Sigma_{22}^d - \Sigma_{11}^d$ vs $t' St$ for different frequency St in steady oscillation. (a) $Re = 0.1$, $k = 45$ ($\Sigma_{22}^d - \Sigma_{11}^d$ scaled by $1/10$). (b) $Re = 1.0$, $k = 200$ ($\Sigma_{22}^d - \Sigma_{11}^d$ scaled by $1/60$).

with the imposed strain, at $St = 20\pi$, indicating a pure elastic response for the interfacial stress. At higher inertia ($Re = 1.0$), we obtain similar behavior at high frequency $St = 20\pi$. But at low and intermediate frequencies, the phase difference δ (between the normal stress $\Sigma_{22}^d - \Sigma_{11}^d$ and the imposed flow strain) reaches a value higher than $\pi/2$ as the frequency is increased before becoming zero at high frequency (Fig. 4).

Expressing $\Sigma_{22}^d - \Sigma_{11}^d = (\Sigma_{22}^d - \Sigma_{11}^d)^0 \sin(t^d St + \delta)$, the nondimensional elastic (storage) and viscous (loss) moduli are

$$\begin{aligned} E_{int}^{d'} &= (\Sigma_{22}^d - \Sigma_{11}^d)^0 St \cos \delta, \\ E_{int}^{d''} &= (\Sigma_{22}^d - \Sigma_{11}^d)^0 St \sin \delta. \end{aligned} \quad (2)$$

The superscript zero represents the amplitude. In Fig. 5, we plot $E_{int}^{d'}$ and $E_{int}^{d''}$ for the same conditions as in Fig. 3. For the low Reynolds number case [Fig. 5(a)], we obtain the classic curves with viscosity dominating elasticity at low frequency and a crossover at intermediate frequencies [14]. The result matches with the analytical models of Oldroyd [15] and Yu and Bousmina [16] (both give identical results in this limit) applicable for Stokes flow. At increased inertia ($Re = 1.0$), we find that for intermediate frequencies the behaviors of the moduli [Fig. 5(b)] are very different from their low Reynolds number counterparts. At very low frequency, the stress is more viscous than elastic. However, with increased frequency, the storage modulus becomes negative. It reaches a minimum value before increasing to become positive. The negative value arises due to $\delta > \pi/2$ in Fig. 4 for the same range of frequency. Both moduli show a maximum that corresponds to a resonance in the drop responses [5]. Note that $Re = 1.0$, $k = Ca^{-1} \sim 100-1000$, and $St = 2-10$ are achievable at a shear

rate of 100 s^{-1} with a $100 \mu\text{m}$ drop of water or alcohol (surface tension $1-10 \text{ dyne cm}^{-1}$).

The phenomenon can be explained by considering the drop as a damped mass-spring system with mass $\hat{\rho}\hat{R}^3$, damping $\hat{\mu}\hat{R}$ (viscosity), and spring $\hat{\Gamma}$ (interfacial tension). \hat{R} is the drop radius. The hat is used to differentiate the model variables from their real counterparts. Under imposed flow forcing $G_0 g(t)$ (proportional to the flow strain rate, G_0 is the magnitude), a measure ζ of the deformation of the drop (assuming an ellipsoidal drop, the difference between its major and minor axes [5]) is governed by an ordinary differential equation (ODE):

$$\begin{aligned} \hat{\rho}\hat{R}^3 \ddot{\zeta} + \hat{\mu}\hat{R} \dot{\zeta} + \hat{\Gamma}\zeta &= \hat{\mu}\hat{R} G_0 g(t) + \hat{\rho}\hat{R}^3 G_0 \dot{g}(t), \\ \dot{\zeta}(0) &= G_0 g(0), \quad \zeta(0) = 0. \end{aligned} \quad (3)$$

The terms on the right-hand side of Eq. (3) mimic the effects of the forcing flow. The first forcing term corresponds to the viscous stress, and the second term represents the dynamic pressure ($\rho \partial u / \partial t \sim \nabla p$). The pressure term

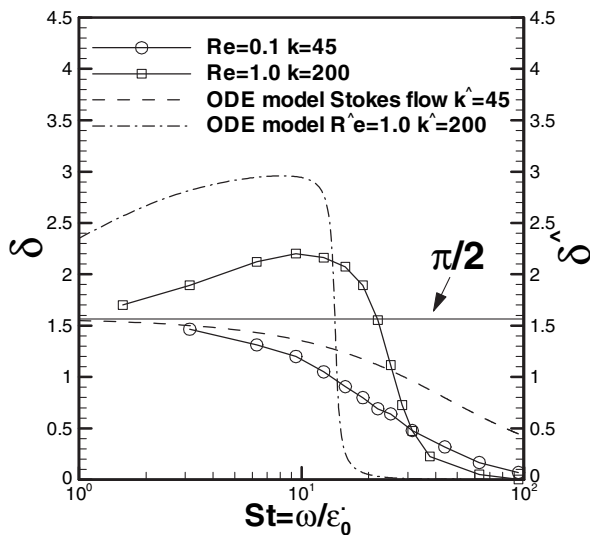


FIG. 4. Phase angle δ between $\Sigma_{22}^d - \Sigma_{11}^d$ and ϵ vs frequency St . The prediction of the one-dimensional model from Eq. (3) is shown in the same plot.

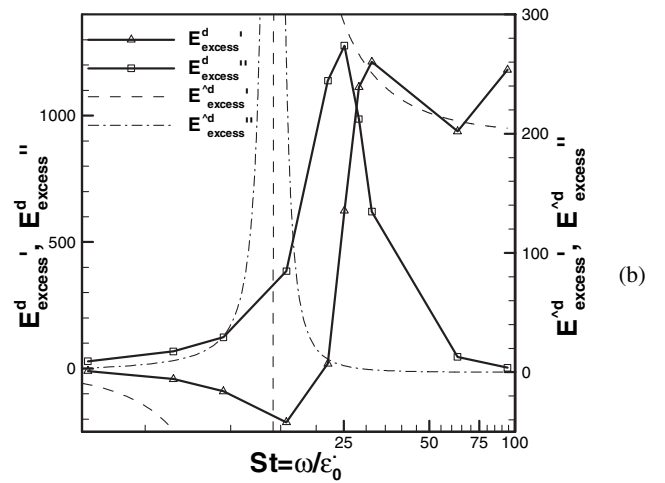
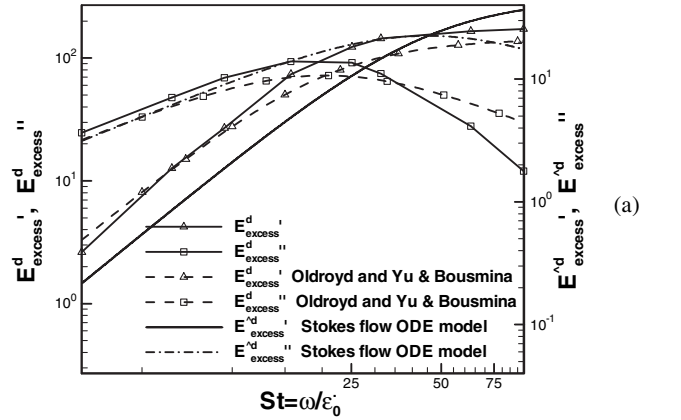


FIG. 5. Nondimensional extensional moduli vs St at (a) $k = 45$, $Re = 0.1$ and (b) $k = 200$, $Re = 1.0$. The predictions of the phenomenological tensor model by Oldroyd and Yu and Bousmina as well as the ODE model are also shown for comparison.

is critical for matching the dynamics of the actual problem. The model can be nondimensionalized using the length scale \hat{R} and time scale \hat{R}/G_0 :

$$\hat{R}e \ddot{\zeta} + \dot{\zeta} + \hat{k}\zeta = g(t) + \hat{R}e \dot{g}(t), \quad \dot{\zeta}(0) = g(0), \quad (4)$$

$$\zeta(0) = 0.$$

where $\hat{R}e = \hat{\rho} \hat{R} G_0 / \hat{\mu}$, $\hat{k} = \hat{\Gamma} / (\hat{\mu} G_0)$, $\hat{S}t = \hat{R} \omega / G_0$. For an oscillating flow $g(t) = \exp(i\omega t)$, the solution is

$$\zeta = \frac{1 + i\hat{R}e \hat{S}t}{\hat{k} - \hat{R}e \hat{S}t^2 + i\hat{S}t} \exp(it' \hat{S}t),$$

$$|\zeta| = \sqrt{\frac{1 + \hat{R}e^2 \hat{S}t^2}{(\hat{k} - \hat{R}e \hat{S}t^2)^2 + \hat{S}t^2}}, \quad (5)$$

$$\hat{\beta} = \tan^{-1} \frac{\hat{S}t}{\hat{k}} (1 - \hat{k} \hat{R}e + \hat{S}t^2 \hat{R}e^2),$$

where $\hat{\beta}$ is the phase lag of the drop response behind the imposed strain rate. The difference of interface tensor principle axes $q_{11-22} = q_{11} - q_{22} \sim \zeta$ [see Eq. (1)]. Therefore $\Sigma_{22}^d - \Sigma_{11}^d = -k(q_{22} - q_{11}) \sim \hat{k}\zeta$. The analogue for the stress-strain phase angle is $\hat{\delta} = \frac{\pi}{2} - \hat{\beta} = \frac{\pi}{2} - \tan^{-1} \frac{\hat{S}t}{\hat{k}} (1 - \hat{k} \hat{R}e + \hat{S}t^2 \hat{R}e^2)$. The loss and the storage moduli therefore are

$$\hat{E}_{\text{excess}}^d{}' = \hat{k} |\zeta| \hat{S}t \cos \hat{\delta}, \quad \hat{E}_{\text{excess}}^d{}'' = \hat{k} |\zeta| \hat{S}t \sin \hat{\delta}. \quad (6)$$

Note that this model is only qualitative and may not quantitatively compare with the simulation. However, it contains the essential physics, and therefore describes the observed trends in phase, the negative and positive values of storage modulus as shown in both Figs. 4 and 5. From Eq. (3), the effects of inertia (Re) are clear. Furthermore, the second term on the right-hand side of Eq. (3) [also the third term in the expression Eq. (5) for $\hat{\beta}$] representing the effect of dynamic pressure is critical in switching from negative to positive value of the storage modulus at higher frequency. In Eq. (5), $\hat{\beta}$ becomes negative due to the term $-\hat{k}\hat{R}e$ making $\hat{\delta} = \pi/2 - \hat{\beta}$ more than $\pi/2$. With a further increase in frequency, the term $\hat{S}t^2 \hat{R}e^2$ becomes dominant, switching the sign of the elastic modulus back. The position and the shape of the peaks due to resonance are also captured well by the model [Fig. 5(b)]. The model peaks are much sharper. The similarity with negative refraction in optical materials mentioned before is demonstrated by the Drude-Lorentz model [6] that contains an element response such as Eq. (5). Both the mechanical and the optical phenomena are dependent on the frequency. Recently, in steady shear negative normal stresses were measured for attractive emulsion [8] and suspension of non-Brownian multiwalled carbon nanotubes [9]. In both cases interaction between elements (drops or nanotubes) play a critical role and form cylindrical aggregates aligned along the vorticity direction. In contrast, we consider a dilute emulsion with negligible interactions where the

negative elastic modulus results from inertial effects of the drop response to the imposed strain rate. In a concentrated emulsion, interactions would lead to additional normal stress due to structure formation. The numerical method used here can simulate such interaction albeit at a substantially more computational cost. Note that emulsion containing viscoelastic drops would have additional physics in droplet response [17]. Instability in high-aspect ratio elastic filament has been theoretically analyzed to predict a negative first normal stress difference for a sheared dilute suspension of such filaments [18].

-
- [1] C.L. Tucker and P. Moldenaers, *Annu. Rev. Fluid Mech.* **34**, 177 (2002); R. G. Larson, *The Structure and Rheology of Complex Fluids* (Oxford University Press, New York, 1999).
 - [2] G.I. Taylor, *Proc. R. Soc. A* **138**, 41 (1932); **146**, 501 (1934).
 - [3] J.M. Rallison, *Annu. Rev. Fluid Mech.* **16**, 45 (1984); H. A. Stone, *Annu. Rev. Fluid Mech.* **26**, 65 (1994); W. Yu and M. Bousmina, *J. Rheol. (N.Y.)* **47**, 1011 (2003); W. Yu *et al.*, *J. Rheol. (N.Y.)* **48**, 417 (2004); P.L. Maffettone and F. Greco, *J. Rheol. (N.Y.)* **48**, 83 (2004); P.L. Maffettone and M. Minale, *J. Non-Newtonian Fluid Mech.* **78**, 227 (1998); E.D. Wetzel and C.L. Tucker, *Int. J. Multiphase Flow* **25**, 35 (1999); *J. Fluid Mech.* **426**, 199 (2001); Y. Wu *et al.*, *J. Non-Newtonian Fluid Mech.* **102**, 281 (2002).
 - [4] G.K. Batchelor, *J. Fluid Mech.* **41**, 545 (1970).
 - [5] X. Li and K. Sarkar, *Phys. Fluids* **17**, 027103 (2005).
 - [6] V.G. Veselago, *Sov. Phys. Usp.* **10**, 509 (1968); J.B. Pendry *et al.*, *IEEE Trans. Microw. Theory Tech.* **47**, 2075 (1999); J.B. Pendry and D.R. Smith, *Phys. Today* **57**, No. 6, 37 (2004).
 - [7] G. Kiss and R. S. Porter, *J. Polym. Sci., Polym. Symp. E* **65**, 193 (1978); L.G. Marucci and P.L. Maffettone, *Macromolecules* **22**, 4076 (1989).
 - [8] A. Montesi *et al.*, *Phys. Rev. Lett.* **92**, 058303 (2004).
 - [9] S. Lin Gibson *et al.*, *Phys. Rev. Lett.* **92**, 048302 (2004).
 - [10] X. Li and K. Sarkar, *J. Rheol.* **49**, 1377 (2005).
 - [11] B.J. Bentley and L.G. Leal, *J. Fluid Mech.* **167**, 219 (1986); **167**, 241 (1986).
 - [12] G. Tryggvason *et al.*, *J. Comput. Phys.* **169**, 708 (2001); K. Sarkar and W.R. Schowalter, *J. Fluid Mech.* **436**, 177 (2001).
 - [13] M. Doi and T. Ohta, *J. Chem. Phys.* **95**, 1242 (1991); J. Mellema and M. W. M. Willemsse, *Physica (Amsterdam)* **122A**, 286 (1983); A. Onuki, *Phys. Rev. A* **35**, 5149 (1987).
 - [14] X. Li and K. Sarkar, *J. Non-Newtonian Fluid Mech.* **128**, 71 (2005).
 - [15] J.G. Oldroyd, *Proc. R. Soc. A* **218**, 122 (1953); **232**, 567 (1955).
 - [16] W. Yu and M. Bousmina, *J. Rheol. (N.Y.)* **46**, 1401 (2002).
 - [17] K. Sarkar and W.R. Schowalter, *J. Non-Newtonian Fluid Mech.* **95**, 315 (2000).
 - [18] L.E. Becker and M.J. Shelley, *Phys. Rev. Lett.* **87**, 198301 (2001).